Gait Generation Through a Feature Based Linear Periodic Function

Avinash Ranganath[1] and Luis Moreno[2]

***Abstract*— By considering locomotion as a set of coordinated oscillations, a method for generating a wide variety of periodic linear gait trajectories is proposed. The shape of the generated trajectory can be defined as a set of features such as symmetry, skewness, signal width, duality and squareness, along with amplitude, offset, phase and frequency parameters. Taking previously proven nonlinear bipedal gait trajectories as reference, a set of linear approximates are modeled, and is tested on a simulated humanoid robot. Then, gait trajectories for producing stable and faster bipedal gait on the same humanoid robot are learned using Genetic Algorithm, through a bottom-up approach.**

***Index Terms*— Bipedal gait, Periodic function, Humanoid, Genetic Algorithm**

I. INTRODUCTION

Humanoid locomotion is an ongoing topic in robotics. Many approaches have been studied. Some make use of reduced models to obtain the dynamics [4], [15], [3], [8] while others prefer a distributed mass formulation [10], [16], [5]. While many of these works are based on Zero Moment Point (ZMP) controllers, an interesting approach is based on the Central Pattern Generator (CPG) method. It has been hypothesized that during animal locomotion, there is a feed-forward mechanism that activates the muscles using signals generated by the CPG, which is located in the spinal cord. The most interesting property of CPG is that it produces a periodic pattern based on simple oscillations.

CPG based techniques have been successfully implemented in humanoid robots [14], [2]. In [12], a CPG controller is combined with a ZMP controller, to obtain a stable bipedal gait. In [13], the authors proposed a CPG controller optimized by Genetic Algorithm (GA). The fitness function contains terms related to ZMP to ensure the stability. [11] presents an approach where a CPG controller generates stable bipedal locomotion trajectories based on human demonstrations.

Several other approaches try to obtain prerecorded data from human bipedal walking and then transfer the locomotion behavior to the robot. Some examples are inverse optimal control [7], reinforcement learning [9] and gait parameter adaptation [6].

In this work we propose a linear gait trajectory generator, which can generate a wide range of linear periodic trajectories. The shape of the generated trajectory is defined as a set of features. In the current work, the trajectories are modeled based on stable gait trajectories generated using the cart-table method, by [3].

In the next section, the linear gait trajectory generator (*Triangle/Square Wave*), and all its individual features, are explained. Experimental results are presented in section three and discussion in sections four. Finally, conclusions are provided in the fifth section.

II. TRIANGLE/SQUARE WAVE MODEL

Looking at locomotion as a set of coordinated oscillations, the objective of this work is to develop a general periodic function, that can produce a wide range of trajectories.

As a starting point, the range of joint trajectories generated using the cart-table method (Fig. 1 and 2) by [4], [3], which is tested and stable, is considered. These trajectories are nonlinear and varied. Taking into account all the different features of the trajectories, a model that can approximately fit these trajectories is developed. In the following subsections, the trajectory of the right hip joint (in the pitch dimension) is considered as reference, and the process of incrementally developing a model, one feature at a time, that fits this trajectory is being explained.

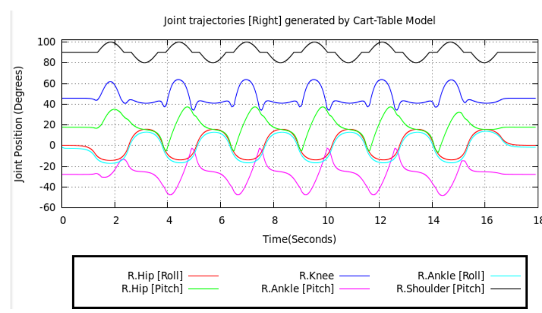

Fig. 1. Joint trajectories of the right hip, knee, ankle and shoulder joints generated based on the cart-table method.

A. Asymmetric Triangle Wave

$$\text{saw}(t) = 2\left(\frac{t}{p} + \frac{\phi}{2\pi} - \left\lfloor \frac{1}{2} + \frac{t}{p} + \frac{\phi}{2\pi} \right\rfloor\right) \tag{1}$$

$$\begin{aligned} \text{tri}(t) = \frac{A}{2}\Bigg(& \left(\frac{\text{saw}(t)}{\chi}\right)(\text{sgn}(\chi - |\,\text{saw}(t)|) + 1) \\ & + \frac{1}{1-\chi}((1-\text{saw}(t))(\text{sgn}(\text{saw}(t) - \chi) + 1) \\ & + (-1-\text{saw}(t))(\text{sgn}(-\text{saw}(t) - \chi) + 1))\Bigg) + O \end{aligned} \tag{2}$$

[1]Avinash Ranganath is a research assistant at the Department of Systems Engineering and Automation, University Carlos III of Madrid, Leganes 28911, Spain `arangana@ing.uc3m.es`

[2]Luis Moreno is a professor at the Department of Systems Engineering and Automation, University Carlos III of Madrid, Leganes 28911, Spain `moreno@ing.uc3m.es`

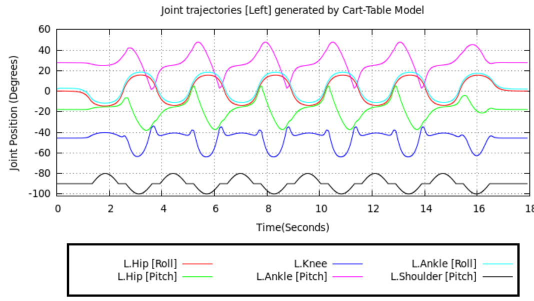

Fig. 2. Joint trajectories of the left hip, knee, ankle and shoulder joints generated based on the cart-table method.

where A ($A \in \mathbb{R}$) is the amplitude, O ($O \in \mathbb{R}$) is the offset, ϕ ($-180^\circ \leq \phi \leq 180^\circ$) is the phase, p ($p \geq 0$) is the period and χ ($0 < \chi < 1$) is the symmetry parameter.

A sawtooth wave function is defined by (1). A triangle wave function, as a combination of sawtooth wave and reverse sawtooth wave ($-saw(t)$), is defined by (2), where parameter χ defines the symmetry of the resulting triangle wave. If $\chi = 0.5$, then the resulting triangle wave is symmetric, else if $0 < \chi < 0.5$ or if $0.5 < \chi < 1$ then the resulting triangle wave tends to lean towards sawtooth wave and reverse sawtooth wave forms, respectively (Fig. 3).

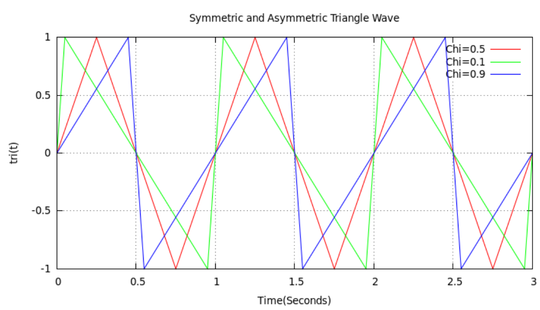

Fig. 3. Triangle waves with $\chi = 0.5$ (red), $\chi = 0.1$ (green) and $\chi = 0.9$ (blue).

The original trajectory and an approximate fit of it based on the triangle wave function, is as shown in Fig. 4. The 5 parameters, which are hand-tuned, of this approximate fit are: $A = 21.28^\circ$, $O = 16.08^\circ$, $\phi = 0^\circ$, $p = 2.56s$ and $\chi = 0.2$.

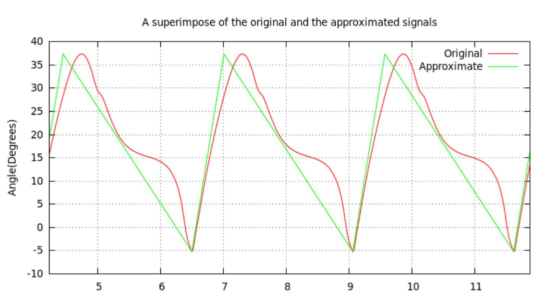

Fig. 4. Original trajectory and the triangle wave based approximate fit.

B. Dual Triangle Wave

From Fig. 4, the simplicity of the triangle wave-based model is quite evident. By tuning the χ parameter, only one of the two halves, either the top or the bottom half, of the original signal can be modeled. So, the current model is extended by considering the two halves independently in the following way:

$$\begin{aligned}\mathrm{tri}(t,\chi) = \frac{1}{2}\Bigg(&\left(\frac{\mathrm{saw}(t)}{\chi}\right)(\mathrm{sgn}(\chi - |\mathrm{saw}(t)|)+1) \\ &+ \frac{1}{1-\chi}((1-\mathrm{saw}(t))(\mathrm{sgn}(\mathrm{saw}(t)-\chi)+1) \\ &+ (-1-\mathrm{saw}(t))(\mathrm{sgn}(-\mathrm{saw}(t)-\chi)+1))\Bigg)\end{aligned} \tag{3}$$

$$y(t) = O + \sum_{i=0}^{1} \frac{A_i}{2} \left|\mathrm{sgn}(\mathrm{tri}(t,\chi_i)) + (-1)^i\right| \mathrm{tri}(t,\chi_i) \tag{4}$$

where $A_i \in \{A_0, A_1\}$ is a pair of amplitudes and $\chi_i \in \{\chi_0, \chi_1\}$ is a pair of symmetry parameters.

In (4), the top half of one triangle wave and the bottom half of another triangle wave (dual triangles), each with independent amplitude and symmetry parameters, are combined together to produce trajectories that have independent halves (top and bottom). Some example trajectories could be seen in Fig. 5.

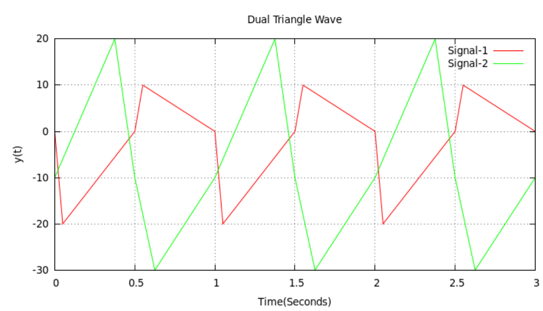

Fig. 5. Triangle waves with asymmetry between the top and bottom halves.

Fig. 6 contains the original trajectory and an approximate fit based on the dual triangle waves model. The 7 hand-tuned parameters are: $A_0 = A_1 = 21.28^\circ$, $O = 16.08^\circ$, $\phi = 0^\circ$, $p = 2.56s$, $\chi_0 = 0.4$ and $\chi_1 = 0.2$.

C. Width Modulation

The dual triangle wave-based approximate fits the original trajectory much closer than the triangle wave model does, but there still exists a discrepancy between the two. The linear model is further enhanced by adding the duty cycle feature, as follows:

$$\begin{aligned}\mathrm{pulse}(t) = \sum_{i=0}^{1}\left(\frac{1-D_i}{2D_i} - \frac{(-1)^i\,\mathrm{saw}(t)}{D_i}\right)&\left\lceil |\mathrm{saw}(t)| - \frac{1-D_i}{2}\right\rceil \\ \times \left\lfloor |\mathrm{saw}(t)| - \frac{1+D_i}{2}\right\rfloor &\left(\frac{\mathrm{sgn}(\mathrm{saw}(t)+(-1)^i)}{2}\right)\end{aligned} \tag{5}$$

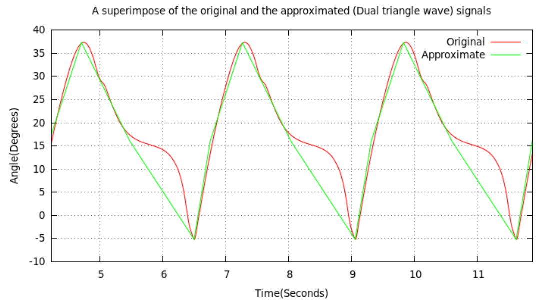

Fig. 6. Original trajectory and the dual triangle wave based approximate fit.

$$\begin{aligned}\operatorname{tri}(t,\chi) = \frac{1}{2}\Bigg(&\left(\frac{\operatorname{pulse}(t)}{\chi}\right)(\operatorname{sgn}(\chi - |\operatorname{pulse}(t)|)+1)\\&+\frac{1}{1-\chi}((1-\operatorname{pulse}(t))(\operatorname{sgn}(\operatorname{pulse}(t)-\chi)+1)\\&+(-1-\operatorname{pulse}(t))(\operatorname{sgn}(-\operatorname{pulse}(t)-\chi)+1))\Bigg)\end{aligned} \tag{6}$$

where $D_i(0 < D_i \leq 1) \in \{D_0, D_1\}$ is a pair of duty cycle parameters.

In (5), the width of a sawtooth wave, within a period, is modulated. If $0 < D_0 < 1$, then the width of the top half of the sawtooth wave is shrunk inversely proportional to the parameter D_0. Similarly, parameter D_1 determines the width of the bottom half of the sawtooth wave. In (6), width-modulated sawtooth and reverse sawtooth waves are combined together to produce a width-modulated triangle wave. An example of this is as seen in Fig. 7.

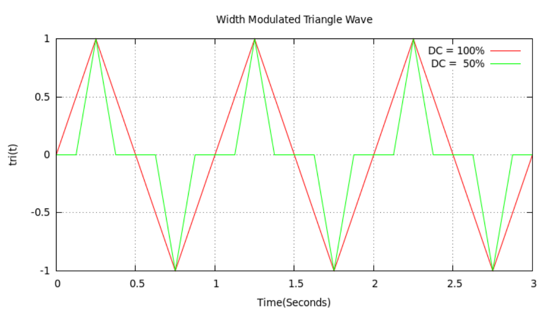

Fig. 7. Triangle waves with duty cycle of 100% (red) and 50% (green).

D. Skewness

$$\begin{aligned}\operatorname{pulse}(t) = \sum_{i=0}^{1} -\frac{(-1)^i}{D_i}&\left(\operatorname{saw}(t) - (-1)^i\left(\frac{1-D_i}{2}\right)(1-\gamma_i)\right)\\&\times\left\lceil |\operatorname{saw}(t)| - \frac{1-D_i}{2}(1+\gamma_i)\right\rceil \Big\lfloor |\operatorname{saw}(t)|\\&\quad - \frac{1-D_i}{2}(1+\gamma_i)\Big\rfloor \left(\frac{\operatorname{sgn}(\operatorname{saw}(t)+(-1)^i)}{2}\right)\end{aligned} \tag{7}$$

where $\gamma_i(-1 \leq \gamma_i \leq 1) \in \{\gamma_0, \gamma_1\}$ is a pair of skewness parameters.

The position, over the x-axis (time), of a width-modulated triangle, within a period, can also be modulated by introducing the skewness factor into (5) as defined in (7).

Parameter γ_0 in (7) determines the position of the upper width-modulated triangle, on the x-axis. If $0 < \gamma_0 \leq 1$ then the triangle is positively skewed, else if $-1 \leq \gamma_0 < 0$ then the triangle is negatively skewed, else if $\gamma_0 = 0$ then the triangle is not skewed. Similarly, parameter γ_1 determines the skewness of the bottom triangle. The value of the γ_i determines the skewness of the triangle, and is only a factor if the triangle has a modulated width (i.e. if $0 < D_i < 1$). If the triangle has a duty cycle of 100%, then γ_i has no effect on the resulting triangle. An example of this is as seen in Fig. 8.

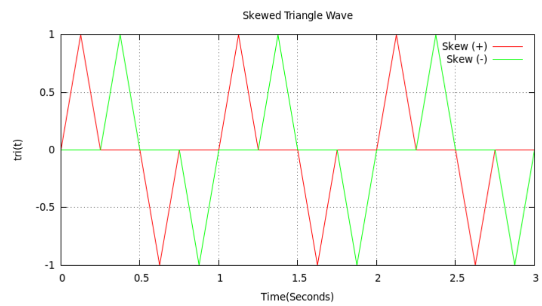

Fig. 8. Width-modulated triangle waves with positive skew (red) and negative skew (green).

The original trajectory in comparison with the approximate fit generated from the updated model is as seen in Fig. 9. The 11 hand-tuned parameters are: $A_0 = A_1 = 21.28°$, $O = 16.08°$, $\phi = 0°$, $p = 2.56s$, $\chi_0 = 0.4$, $\chi_1 = 0.35$, $D_0 = 1.0$, $D_1 = 0.55$, $\gamma_0 = 0$ and $\gamma_1 = -1.0$.

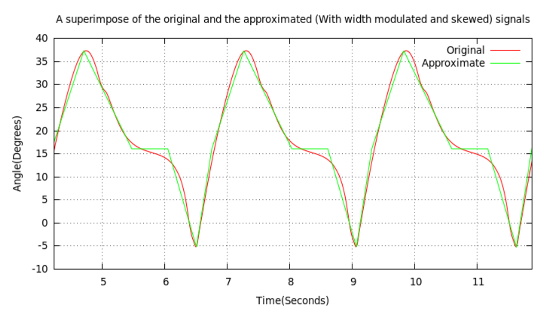

Fig. 9. Original trajectory and the approximate fit based on the model with duty cycle and skewness factors.

E. Squareness

The updated approximation with modulated width and skewness factors fits the original trajectory much better compared to the previous model. The linear model is further enhanced by adding the squareness factor as follows,

$$A_i' = \frac{A_i}{1-\varepsilon_i} \tag{8}$$

$$y(t) = O + \sum_{i=0}^{1} A'_i \left| \frac{\operatorname{sgn}(\operatorname{tri}(t,\chi_i)) + (-1)^i}{2} \right| \times \Big(\operatorname{sgn}(\varepsilon_i) \lfloor |\operatorname{tri}(t,\chi_i)| + \varepsilon_i \rfloor (1-\varepsilon_i)(-1)^i - (\lceil |\operatorname{tri}(t,\chi_i)| + \varepsilon_i \rceil - 2) \operatorname{tri}(t,\chi_i) \Big) \quad (9)$$

where $\varepsilon_i (0 \le \varepsilon_i < 1) \in \{\varepsilon_0, \varepsilon_1\}$ is a pair of squareness parameters.

In (9) ε_i determines how square or triangular the signal is. If $\varepsilon_0 = 0$ then the upper half is of a perfect triangular shape, else if $0 < \varepsilon_0 < 1$, then the top part of the upper half of the signal is clipped, and the signal is resized by increasing the amplitude parameter in proportion as defined in (8). The magnitude of the ε_0 parameter determines the squareness of the signal. Similarly, ε_1 determines the squareness of the bottom half of the signal. Some examples are as seen in Fig. 10.

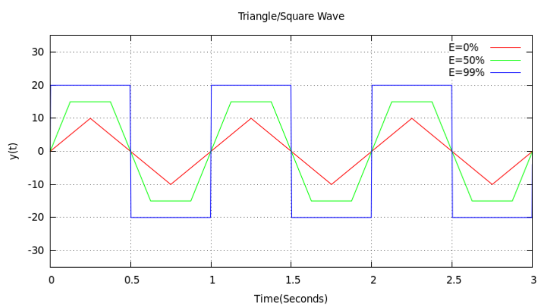

Fig. 10. Trajectories with triangular (red), semi-triangular (green) and square wave forms.

The new linear approximate fit, with squareness factor included, compared to the original signal is as shown in Fig. 11. The 13 hand-tuned parameters are: $A_0 = A_1 = 21.28°$, $O = 16.08°$, $\phi = 0°$, $p = 2.56s$, $\chi_0 = 0.4$, $\chi_1 = 0.35$, $D_0 = 1.0$, $D_1 = 0.55$, $\gamma_0 = 0$, $\gamma_1 = -1.0$, $\varepsilon_0 = 0.1$ and $\varepsilon_1 = 0.05$.

Fig. 11. Original trajectory and the approximate fit based on the model with squareness factor.

Similarly to the right hip joint trajectory, an approximate linear fit to the original trajectory of right knee joint was modeled, and is as shown in Fig. 12. The 13 hand-tuned parameters for this approximate model are: $A_0 = 28.72°$, $A_1 = -6.72°$, $O = 35.02°$, $\phi = 0°$, $p = 2.56s$, $\chi_0 = \chi_1 = 0.5$, $D_0 = 0.8$, $D_1 = 1.0$, $\gamma_0 = \gamma_0 = 0$, $\varepsilon_0 = 0.4$ and $\varepsilon_1 = 0.95$.

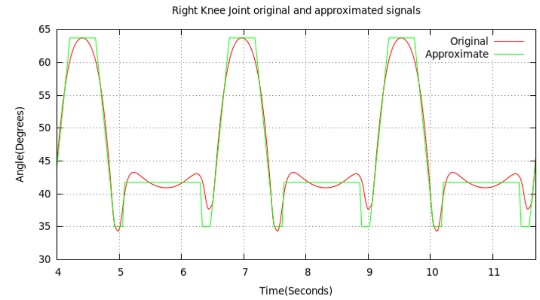

Fig. 12. Right knee joint: The original trajectory and an approximate linear fit.

III. Experimental Results

A. Modeled Controller

Similar to right hip and right knee joints, the remaining 10 joint trajectories (Fig. 1 and 2) are modeled approximately by hand-tuning the parameters. The resulting trajectories are tested on the simulated model of the small-sized ($60cm$) humanoid robot HOAP-3, in an ODE-based physics simulator OpenRAVE [1].

The robot starts from a stand-still position, where all the joints are at $0°$. Since all 12 joint trajectories oscillate at a non-zero center amplitude (i.e. $O_j \neq 0$), a sudden displacement of the joint positions at time $t = 0 + \Delta t$ perturbs the Center Of Gravity (COG) of the robot, and results in the robot loosing balance. To overcome this, joint trajectories are modified to crescendo to full intensity very slowly, using the following stabilization filter:

$$y(t) = \begin{cases} y(t)\frac{t}{\tau}, & \text{if } t < \tau \\ y(t), & \text{otherwise} \end{cases}$$

where $\tau > 0$ is the stabilization period parameter.

Parameter τ defines the period, starting from time $t = 0$, during which the joint trajectory linearly increase in intensity, starting from the initial joint position of $0°$ (Fig. 13). In this experiment, stabilization period for all the joint controllers are set to $\tau_j = 30s$.

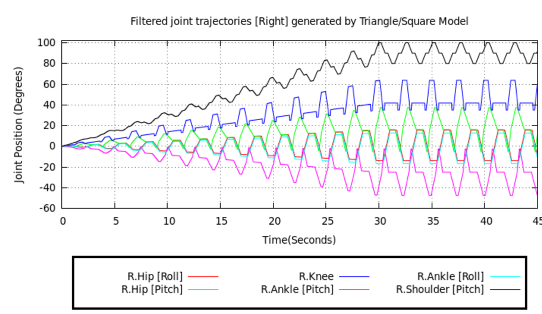

Fig. 13. Joint trajectories generated by *Triangle/Square* model crescendo starting from $t = 0s$.

The modified trajectories, which are pre-generated, are evaluated on the simulated robot, and 90% of the evaluations resulted in a stable bipedal walking gait. The hip, knee, ankle and shoulder joints all start to oscillate slowly, while increasing in intensity at every time step ($\Delta t = 2ms$). At around $t = 15s$, the robot starts to take the first couple of very small steps backwards, as the torso gradually leans forward at the same time. Then at around $t = 20s$, the robot takes a big step forward, compensating for the forward lean, and within the next 2 to 3 steps, the robot stabilizes its balance, and enters into a rhythmic cycle. Then, the robot continues to walk in a stable gait, at an average walking speed of $8cm/s$ until the end of the evaluation (a period of $300s$). Screen capture of one gait cycle of the stable gait is as shown in Fig. 14 [1].

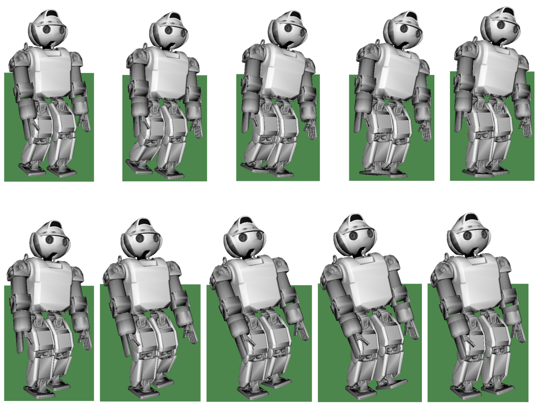

Fig. 14. Screen capture of one gait cycle during stable bipedal gait, starting from top-left and ending at bottom-right, one row at a time.

In the failed evaluations (10%) the robot does usually loose its balance at around $t = 20s$, as it tries to enter a stable gait cycle. Although the reference joint trajectories are the same for all the evaluations, the robot fails to enter a stable gait cycle on instances, because of the stochasticity modeled in the simulation environment, combined with the fact that the linear trajectories are only an approximate of the original.

B. Learned Controller

The natural next step in the research is to evaluate the proposed controller by learning the control parameters through a bottom-up approach, with minimum or no modeling at all. The objective is to learn control parameters for generating stable bipedal gait on the simulated HOAP-3 robot, with as minimum modeling of the robot as possible. Genetic Algorithm (GA) is used for optimizing the control parameters, wherein the speed of locomotion is used as the fitness function. The HOAP-3 robot has 28 joints in total, of which only 10 joints, that are relevant for locomotion, are controlled, while the rest of the joints are maintained at a constant default position.

To produce a meaningful gait, p, the period parameter, has to be a common value for all the joints, although needing to be optimized. Considering this, the total number of parameters, including one τ parameter per joint, that needs to be optimized would be $10 \times 13+$ a common p parameter $= 131$ parameters, making it a search problem in a 131 dimensional space. To reduce the dimension of the search space, the following constraints are applied,

- In bipedal walking gait, there exists a symmetry between the respective joints of the two legs, such that $y_{Right_j}(t) = -y_{Left_j}(t)$, and $|\phi_{Right_j} - \phi_{Left_j}| \approx 180^\circ$, where $\forall j \in J$, $J = \{HipRoll, HipPitch, Knee, AnklePitch, AnkleRoll\}$. That is, the joint angles of respective left and right leg joints, at time t, are opposite of each other along with an approximate phase difference of 180° between them. Taking advantage of this, the dimension of the search space can be reduced by a factor of 2 from 131 dimensions to 66 dimensions, by modeling the joint trajectories of all the joints of one leg based on the respective joint trajectories of the other leg.
- In bipedal walking gait, there also exists a symmetry between the shapes of hip roll and ankle roll joint trajectories of each leg, varying only in amplitude. This feature can be used to further reduce the search space, by modeling the ankle roll joint over the hip roll joint, such that the only parameters needed to be optimized for the ankle roll joint are the amplitude parameters A_0 and A_1, further reducing the dimension of the search space from 66 dimensions down to 55 dimensions.
- Based on the kinematic model of the robot, the range of some control parameters such as amplitude and offset, and that of the τ parameter are reduced, resulting in narrowing the width of the search space. Control parameters are optimized in the range as presented in Table I.

TABLE I
RANGE OF CONTROL PARAMETERS USED WHILE OPTIMIZATION

Parameters	*Minimum*	*Maximum*
A_0	0°	35°
A_1	-10°	30°
O	-30°	50°
ϕ	-180°	180°
p	$0.6667s$	$5s$
χ_0, χ_1	0.01	0.99
D_0, D_1	0.01	1.0
γ_0, γ_1	-1.0	1.0
$\varepsilon_0, \varepsilon_1$	0	0.99
τ	$7s$	$17s$

A standard GA approach is followed, using Roulette Wheel selection method and Intermediate Recombination method for reproducing new offspring. Table II contains the GA parameters employed.

Fig. 15 plots the fitness value of the best candidate and average fitness of the population at the end of each generation. At the end of the evolution, the optimized controller is able to produce a very stable bipedal walking gait, with a success rate of 100%, at a speed of $14cm/s$, compared to the average speed of $8cm/s$ achieved by the modeled controller.

[1]Video at: `http://youtu.be/5FWjN_2mW8s`

TABLE II

GA PARAMETER VALUES USED FOR EVOLUTION

Parameters	*Value*
Population size	200
Genome size	55
Evaluation period	50 seconds
Evolution length	23 generations
Crossover rate	50.0%
Elite population	12.5%
Mutation rate	1/Size of genome

The evolved gait has a low period value of $p = 1.37s$. The robot takes small but quick steps, barely lifting the feet off the ground, which ensures stability, while the low period value result in faster walking gait. Average step length of the evolved gait is $3.1cm$ with a standard deviation of $1.86cm$, while the average step length of the modeled gait is $4.92cm$ with a standard deviation of $1.52cm$.

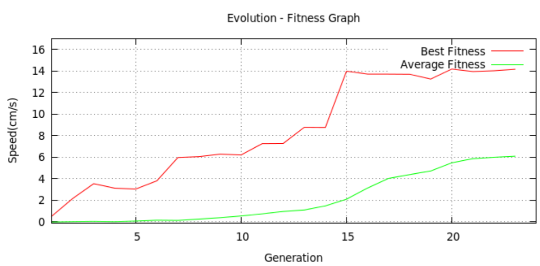

Fig. 15. Graph showing the fitness value of best individual and average fitness value of the population during evolution.

IV. DISCUSSION

The objective of this work is to develop a linear periodic function that is feature-based, relatively simple and that can produce a wide range of trajectories for locomotion. As a first step, the validity of the proposed controller was tested by creating an approximate of a previously known stable trajectory. The COG of the robot is not explicitly considered while modeling the approximate trajectories, but is implicit since the reference trajectories are modeled based on this consideration. All 13 parameters of each trajectory generator are hand-tuned to model the reference trajectories as close as possible, but a least squares method can be used too as an alternate. The hand tuned controller was able to produce a stable bipedal walking gait, validating the viability of the proposed controller.

Then, as a second step, the control parameters are learned in a bottom-up approach, based only on the stability and speed of the resulting gait. GA is used for optimizing the control parameters, during which, candidate controllers resulting in the robot falling over at any point during the evaluation are give a fitness value of 0. This results in exerting selective pressure towards candidate solutions that do not fall over, albeit moving very little during the early part of the evolution. At the end, the evolution process is able to produce a gait that is very stable, with a success rate of 100%, and 75% faster than the gait produced by the trajectories based on the cart-table method, further validating the viability of the proposed controller.

The proposed model can also be used as an online controller for producing gaits, both in humanoids and other legged robots. It can also be used as a lower-level controller within a larger framework, wherein another higher-level controller could modulate the lower-level controller's parameters, based on sensory inputs for maintaining balance, avoiding obstacles, etc. Since the proposed model is feature-based, depending on the complexity of the robot and/or the gait, certain features of the periodic function can either be turned off or kept at a constant, and thereby reducing the number of parameters that needs to be tuned. By compromising the feature that dictates the asymmetry factor between the upper and the lower half of a trajectory, the tunable parameter count per joint can be dropped from 14 down to 10 parameters.

In the current primary version of the proposed model, although the reference trajectories produced are strictly linear, the actual trajectory followed by the joints are nonlinear (Fig. 16). We plan to extend the current model by adding nonlinear features. Also, we plan to evaluate the feasibility of the generated trajectories on the real HOAP-3 humanoid robot in the near future.

The main objective of this work is not only to have a method for generating simplified models of pre-existing gait trajectories, but to create a framework through which stable gait trajectories can be learned from scratch, needing minimum modeling of the robot. Using the proposed controller, we are able to prove that a stable bipedal walking gait can be learned through a model-free bottom-up approach. We are currently working of learning more complex bipedal gaits by involving force sensors and joint encoders in the fitness function.

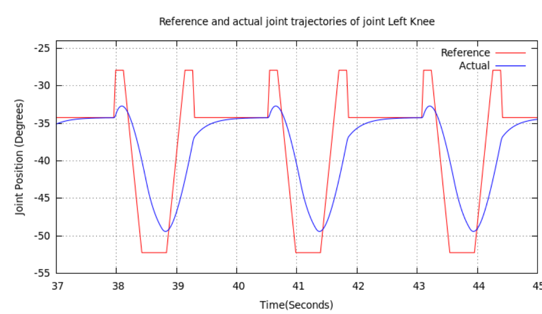

Fig. 16. Reference and actual joint trajectory of the left knee joint, during stable walk.

V. CONCLUSIONS

A feature-based linear periodic function for producing gait trajectories is proposed in this paper. Simple sawtooth waves are combined to form triangle waves, and features such as symmetry, duality, width, skewness and squareness are defined to modulate the resulting trajectories. A linear approximate of a known stable joint trajectory, generated with the cart-table method, is created and evaluated on the simulated version of the HOAP-3 humanoid robot. Experimental results of the hand-tuned controller show a 90% success rate, after joint trajectories are modified by passing through a stabilization filter. Then the control parameters are learned through a bottom-up approach using GA, resulting in a very stable gait that has a success rate of 100% and 75% faster than the modeled controller.

VI. Acknowledgments

The authors would like to thank Miguel González-Fierro and Carlos Balaguer for providing assistance with the cart-table-method-based stable gait trajectories, used in this work as the reference model.

References

[1] R. Diankov and J. Kuffner. Openrave: A planning architecture for autonomous robotics. Technical Report CMU-RI-TR-08-34, Robotics Institute, Pittsburgh, PA, July 2008.

[2] G. Endo, J. Morimoto, T. Matsubara, J. Nakanishi, and G. Cheng. Learning cpg-based biped locomotion with a policy gradient method: Application to a humanoid robot. *The International Journal of Robotics Research*, 27(2):213–228, 2008.

[3] M. González-Fierro, C. Balaguer, N. Swann, and T. Nanayakkara. Full-body postural control of a humanoid robot with both imitation learning and skill innovation. *International Journal of Humanoid Robotics*, 1(04):613–636, 2014.

[4] S. Kajita, F. Kanehiro, K. Kaneko, K. Fujiwara, K. Harada, K. Yokoi, and H. Hirukawa. Biped walking pattern generation by using preview control of zero-moment point. In *Robotics and Automation, 2003. Proceedings. ICRA'03. IEEE International Conference on*, volume 2, pages 1620–1626. Ieee, 2003.

[5] O. Khatib, L. Sentis, J. Park, and J. Warren. Whole-body dynamic behavior and control of human-like robots. *Int. J. of Humanoid Robotics*, 1(1):29–43, 2004.

[6] K. Miura, M. Morisawa, S. Nakaoka, F. Kanehiro, K. Harada, K. Kaneko, and S. Kajita. Robot motion remix based on motion capture data towards human-like locomotion of humanoid robots. In *Humanoid Robots, 2009. Humanoids 2009. 9th IEEE-RAS International Conference on*, pages 596–603. IEEE, 2009.

[7] K. Mombaur, A. Truong, and J. Laumond. From human to humanoid locomotion—an inverse optimal control approach. *Autonomous robots*, 28(3):369–383, 2010.

[8] C. A. Monje, P. Pierro, T. Ramos, M. González-Fierro, and C. Balaguer. Modelling and simulation of the humanoid robot hoap-3 in the openhrp3 platform. *Cybernetics and Systems*, 44(8):663–680, 2013.

[9] J. Morimoto and C. G. Atkeson. Learning biped locomotion. *Robotics & Automation Magazine, IEEE*, 14(2):41–51, 2007.

[10] K. Nagasaka, H. Inoue, and M. Inaba. Dynamic walking pattern generation for a humanoid robot based on optimal gradient method. In *Systems, Man, and Cybernetics, 1999. IEEE SMC'99 Conference Proceedings. 1999 IEEE International Conference on*, volume 6, pages 908–913. IEEE, 1999.

[11] J. Nakanishi, J. Morimoto, G. Endo, G. Cheng, S. Schaal, and M. Kawato. Learning from demonstration and adaptation of biped locomotion. *Robotics and Autonomous Systems*, 47(2):79–91, 2004.

[12] J. Or. A hybrid cpg–zmp control system for stable walking of a simulated flexible spine humanoid robot. *Neural Networks*, 23(3):452–460, 2010.

[13] J. Shan, C. Junshi, and C. Jiapin. Design of central pattern generator for humanoid robot walking based on multi-objective ga. In *Intelligent Robots and Systems, 2000.(IROS 2000). Proceedings. 2000 IEEE/RSJ International Conference on*, volume 3, pages 1930–1935. IEEE, 2000.

[14] J. Shan and F. Nagashima. Neural locomotion controller design and implementation for humanoid robot hoap-1. In *20th annual conference of the robotics society of Japan*, 2002.

[15] P. Wieber. Trajectory free linear model predictive control for stable walking in the presence of strong perturbations. In *Humanoid Robots, 2006 6th IEEE-RAS International Conference on*, pages 137–142. IEEE, 2006.

[16] K. Yamane and Y. Nakamura. Dynamics filter-concept and implementation of online motion generator for human figures. *Robotics and Automation, IEEE Transactions on*, 19(3):421–432, 2003.